Computers and Concrete, *Vol. 19, No. 5 (2017) 567-577*
DOI: https://doi.org/10.12989/cac.2017.19.5.567

Investigation of the behavior of reinforced concrete hollow-core thick slabs

Adel A. Al-Azzawi* and Sadeq A. Abed[a]

Department of Civil Engineering, Al-Nahrain University, Baghdad, Iraq

(Received October 2, 2016, Revised January 10, 2017, Accepted February 2, 2017)

Abstract. This study presents investigation of the behavior of moderately thick reinforced concrete slabs having hollow cores with different parameters. The experimental part of this investigation includes testing eight specimens of solid and hollow-core slab models having (2.05 m) length, (0.6 m) width and (25 cm) thickness under two monotonic line loads. Load versus deflection was recorded during test at mid span and under load. Numerically, the finite element method is used to study the behavior of these reinforced concrete slabs by using ANSYS computer program. The specimens of slab models are modeled by using (SOLID65) element to represent concrete slabs and (LINK180) element to represent the steel bars as discrete axial members between concrete nodes. The finite element analysis has showed good agreement with the experimental results with difference of (4.71%-8.68%) in ultimate loads. A parametric study have been carried out by using ANSYS program to investigate the effects of concrete compressive strength, size and shape of core, type of applied load and effect of removing top steel reinforcement.

Keywords: experimental; finite element; reinforced concrete; hollow-core slab

1. Introduction

The one way reinforced concrete slab can be done in three forms of slabs: solid slabs, ribbed slabs and hollow-core slabs. Hollow core floors represent a special kind of floor totally made of concrete lightened by leaving longitudinal voids (cores) of suitable size to create webs to reduce weight, costs, as fire resistance and for electrical and mechanical purposes. Primarily, hollow core elements are used as floor or roof deck systems and also have applications as wall panels, sound barriers, spandrel members and bridge deck units. Reinforced concrete hollow-core slab is made with cores in one direction with temporary or permanent formwork according the following points:

1. Cross section of hollow-core slab was defined as continuous of I-section parts and designed as a one way ribbed slab with top and bottom flanges.
2. Conventional span length up to 7 m and width of each panel up to 2.4 m.
3. Assumed moderately thick Plate (thickness to span ratio $\frac{h}{L} = \frac{1}{10} - \frac{1}{5}$).
4. Limitations of cross section according to ACI-318 (2014) code as shown in Fig. 1:
   - $b_w \geq 100$ mm
   - $h_w \leq 3.5\ b_w$
   - $s \leq 800$ mm
   - $h_f \geq s/2$, $h_f \geq 50$ mm
   - $b_f = b_w$+dia. of core
   - b_w: width of web
   - h_w: height of web(diameter of core)
   - h_f: height of flange top or bottom
   - b_f: width of flange

The main objective of this studying is to investigate the behavior of one way reinforced concrete slab with longitudinal hollow cores. Experimental investigation is to be carried out for these types of slabs and solid slabs then the testing results will be compared through changing two parameters, size of core and shear span effective depth (a/d) ratio. Theoretical investigation is to be carried out by using finite element program ANSYS V.15 (2013) to compare the results obtained from the experimental tests. The accuracy of the finite element solution is checked and used to study the effect of some additional parameters on the behavior of slabs.

2. Literature review

Pajari (2004) carried out four tests on pre-stressed hollow core slab units. The slab units, two of them 200 mm thickness with 4 m span and two 400 mm thickness with 6 m span, were subjected to pure torsion and together have 1200 mm width. In all tests the observed failure mode was the same as the predicted one, i.e., cracking of top flange in angle of 45° with the longitudinal axis of the slab unit. The predicted torsional resistance was 60% and 70% of the observed resistance for 200 mm and 400 mm slabs, respectively, when the lower characteristic value for the tensile strength of the concrete was used for prediction.

Chang *et al.* (2008) presented a simple computational method to be used in design and modeling the structural behavior of hollow core concrete slabs in fires. The

*Corresponding author, Assistant Professor
E-mail: dr_adel_azzawi@yahoo.com
[a]M.S. Student
E-mail: sadeq_a.abed@yahoo.com

ISSN: 1598-8198 (Print), 1598-818X (Online)

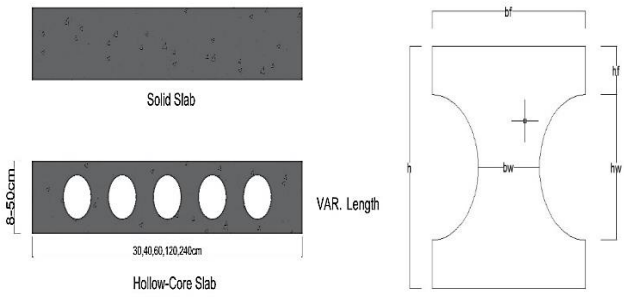

Fig. 1 Dimensions of cross sections of hollow-core slab

Table 1 Reinforced concrete slabs specimens

Slab No.	Type	a/d
Slab-1	Solid slab	2
Slab-2	Solid slab	2.5
Slab-3	Solid slab	3
Slab-4	Hollow-core slab (150 mm core size)	2
Slab-5	Hollow-core slab (150 mm core size)	2.5
Slab-6	Hollow-core slab (150 mm core size)	3
Slab-7	Hollow-core slab (100 mm core size)	2.5
Slab-8	Hollow-core slab (75 mm core size)	2.5

proposed model consists of a grillage system using beam elements to include the thermal expansion in both directions and to simulate the vertical cracking in the flanges, with the topping concrete modeled using shell elements. The simulation outcomes show good agreement with the experimental results.

Hai-tao *et al.* (2011) examined the inner force transfer mechanism of a column-supported cast-in-situ hollow core slab using finite element analysis by (ANSYS) program. The dimensions of the floor system were (21.6×21.6 m) consist from three panels in each direction, each panel (7200×7200 mm) with 300 mm thickness. The diameter of hole was 200 mm and tube filler's length was 900 mm with ribs having 100 mm width between holes. The analysis results of hollow core slab and the corresponding solid slab were compared.

Rahman *et al.* (2012) tested full-scale pre-stressed precast hollow-core slabs with different shear span to depth (a/d) ratio, which were loaded to failure to ascertain the ultimate load-carrying capacity of these slabs. A total of 15 slab specimens, 5 and 2.5 m in span and having three different depths, 200, 250 and 300 mm were tested to failure using four-point load test. It was interesting to note that the failure mode of hollow-core slabs changed from pure flexure mode to flexure-shear mode for slabs with depth greater than 200 mm. The analysis of the experimental results showed that the existing ACI code equations underestimated the flexure-shear strength of these hollow-core slabs.

Brunesi *et al.* (2014) carried out comparison between experimental, analytical and finite element method for shear strength capacity of precast pre-stressed concrete hollow core slabs with (200-500) mm thick without transverse reinforcement through a campaign of detailed nonlinear finite element analysis, matching experiments test data collected by PAJARI from past program. These members (49 specimens) characterized with six nominal slab depths, five hollow shapes with circular and non-circular voids, different voids ratios, several pre-stressing steel strands arrangements and levels of initial pre-stress then comparative with traditional codes. From finite element results, the proposed numerical approach was validated by focusing on a single precast prestressed hollow-core unit.

Haruna (2014) studied the flexural behavior of precast pre-stressed concrete hollow-core units with cast-in-place concrete topping, through load testing of five full-scale specimens. The specimens were divided into two groups wide and narrow. A cast-in-place concrete was cast on top of the hollow-core units selected from the two groups to form a composite system. Presence of cast-in-place topping slab improved the behavior of hollow-core units by increasing the flexural crack initiation and maximum load capacities as well as the stiffness. As a result of premature loss of composite behavior, the predicted load capacity of these specimens assuming a fully composite behavior remained on the non-conservative side. The results obtained in this study suggested that floor system made of cast-in-place concrete topping placed over the machine finished surface of precast concrete hollow-core units with no interfacial roughening is not able to provide the interface shear strength required to develop a fully composite behavior.

Lee (2014) studied the web shear capacity of hollow core slabs (HCS) through a large number of shear tests. The analysis of results indicated that the minimum shear reinforcement requirement for deep HCS members are too severe, and that the web-shear strength equation in ACI 318 code does not provide good estimation of shear strengths for HCS members. Thus, in this paper, a rational web-shear strength equation for HCS members was derived in a simple manner, which provides a consistent margin of safety on shear strength for the HCS members up to 500 mm deep.

Through previous studies, hollow cores are made in prestressed concrete thin slabs while in the present research it is made in normal reinforced concrete thick slabs and the analysis of these hollow core slabs are investigated. In general, the challenge of using hollow cores in slabs was preventing the shear failure of these slabs which may happen due to removing the cores from concrete. Many previous researches were carried out to study the shear behavior of these thin slabs, numerically and analytically but few of them carried experimental investigation for studying the behavior of thick slabs. In this study, the flexural behavior of one way reinforced concrete thick slabs with and without longitudinal cores were adopted experimentally and numerically by creating circular voids at middle plane of cross sections with varying the core diameter and the ratio of shear span to effective depth (a/d).

3. Details of experimental test

Experimental program comprises casting eight small-

Table 2 Properties of materials

Properties of concrete material		
Property	Experimental	ACI318M (2014)
Compressive strength (f'_c) (MPa)	38.1	-
Splitting tensile strength(f'_{ct}) (MPa)	3.4	3.09 ($0.5\sqrt{f'_c}$)
Modulus of rupture (f_r) (MPa)	3.75	3.83 ($0.62\sqrt{f'_c}$)
Modulus of elasticity (E_c) (MPa)	229385.5	29010.8 ($4700\sqrt{f_c'}$) 29926.2 ($W_c^{1.5}0.043\sqrt{f_c'}$)
Properties of steel reinforcement material		
Property	Test results	
Nominal diameter (mm)	8	
Measured diameter (mm)	7.86	
Yield stress (f_y) (MPa)	578.18	
Ultimate stress (f_u) (MPa)	655.74	

scale (1:2) one way solid and hollow-core reinforced concrete thick slab specimens taking into consideration the scaling of steel reinforcement by using half diameter of bar in the slab specimen. Three sizes of circular cores with three different values of shear span effective depth ratio (a/d) (ratio of load position to the effective depth of the slab) was considered in experimental work as shown in Table 1. The aim was to study the flexural and shear behavior of these slabs under two static line loads by using the flexural testing machine.

3.1 Properties of the slab specimens

For the slab specimens, the properties of the hardened concrete and steel reinforcement which used for manufacturing the prototype of these slabs are summarized in Table 2.

The nominal dimensions of slab specimens are (2050 mm) in length with (600 mm) width and (250 mm) thickness. These slabs which have span length (1750 mm) were tested under two line loads with different shear span effective depth ratio (a/d). These contains, three one-way solid slab, three hollow-core slabs with circular core size (150 mm) and another two hollow-core slabs with circular core size (100 mm) and (75 mm). The hollow cores of these slabs are molded by using Poly Vinyl Chloride (PVC) pipes longitudinal through slabs with (2 mm) thickness.

The reinforcement design of all one way reinforced concrete slabs was done according to the design procedure given in ACI 318 (2014) for both solid and hollow-core slabs. The main longitudinal reinforcement consists from 6 bars with (Ø 8 mm) at top and bottom while the secondary transverse reinforcement consists from 14 bar (Ø 8 mm) (with spacing 150 mm) at top and bottom also with concrete cover from all sides 25 mm as shown in Fig. 2.

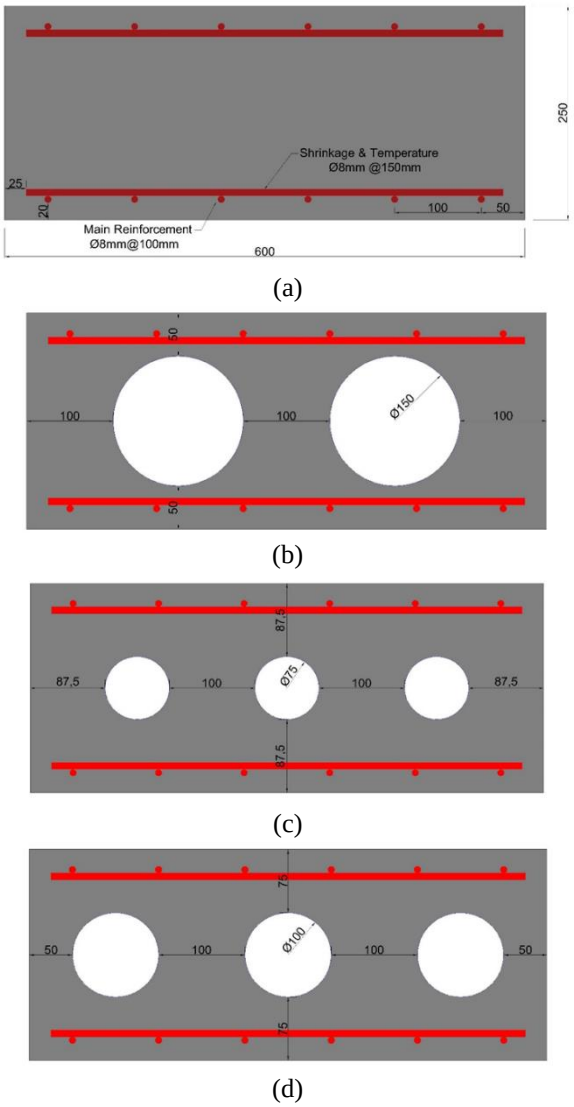

Fig. 2 Cross sections of slabs (a) Solid slab (b), (c) & (d) Hollow-core slab with core diameter (150, 100, 75 mm)

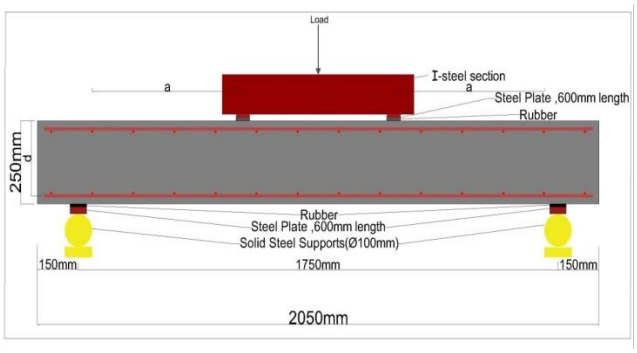

Fig. 3 Details of slab testing

3.2 Testing of the slab specimens

Eight simply supported slab specimens under two line loads were tested by using hydraulic universal testing machine at the Civil Engineering Laboratory/College of Engineering/ Al-Nahrain University. At first, the solid steel circular supports installed with the required span length (1.75 m) from center to center. A steel plate with width (50 mm) were put over the supports and under two line loading with rubber pieces to prevent the crushing of concrete's surface. After installation the specimen over the supports, I-section steel beam was set over the specimen with length (1

(a)

(b)

Fig. 4(a) Photograph of the mold of hollow-core slab, (b) Photograph of hollow-core slab testing setup

m) to apply the two line load as shown in Figs. 3 and 4. The monotonically loading was applied with increased (2.5-5 kN) increments and the central deflection is recorded using the dial-gages and the deflection under the loading points which recorded by the machine. After each increment of loading, the deflection was recorded and monitoring the bottom face of slab. The cracking and ultimate load at failure stage were recorded with the deflections. It is noticed that all remarks were recorded during the test and the developments of cracks (crack pattern) were marked with a pen at each load increment.

4. Material properties and constitutive models

A nonlinear finite element analysis has been carried out to analyze all tested solid and hollow-core slabs. The analysis was performed by using ANSYS release (15.0) computer program by subprogram ANSYS Parametric Design Language (APDL) for structural analysis problems.

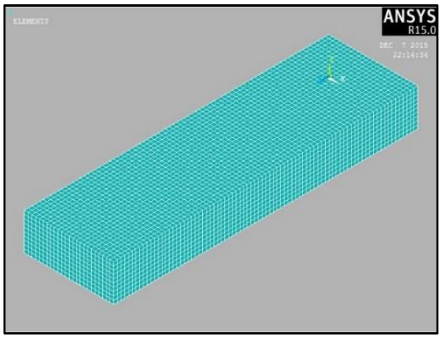

1

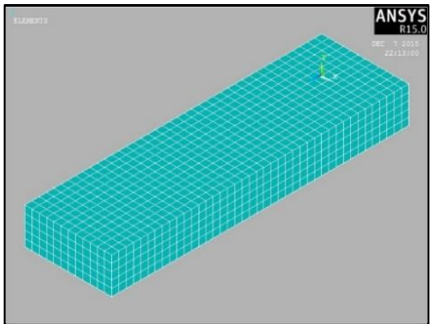

2

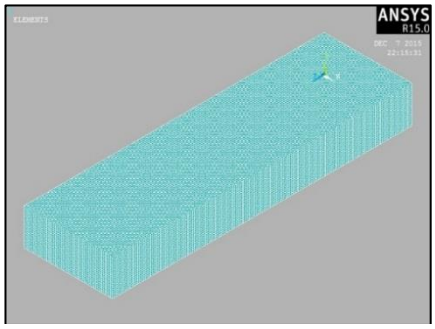

3

Fig. 5 Selecting mesh density of sizes (50, 25 and 12.5 mm)

In the comprehensive sense, any model must comprise all the nodes, elements, boundary conditions, material properties, real constants, and all other features which are used to represent the physical system of the current slab model (ANSYS User's Manual 2013).

4.1 Element type

• SOLID65 element was used to model the concrete and it has eight nodes with three degrees of freedom at each node-translations in the nodal *x*, *y*, and *z* directions. The most important aspect of this element is the treatment of nonlinear material properties. The (SOLID65) element has the capability of plastic deformation, creep, cracking in three orthogonal directions, and crushing in compression.

• LINK180 element was used to model steel reinforcement. This element is a 3D spar element and it has two nodes with three degrees of freedom-translations in the nodal *x*, *y*, and *z* directions. Perfect bond between the concrete and steel reinforcement considered. However, in the present study the steel reinforcing was connected between nodes of each adjacent concrete solid element

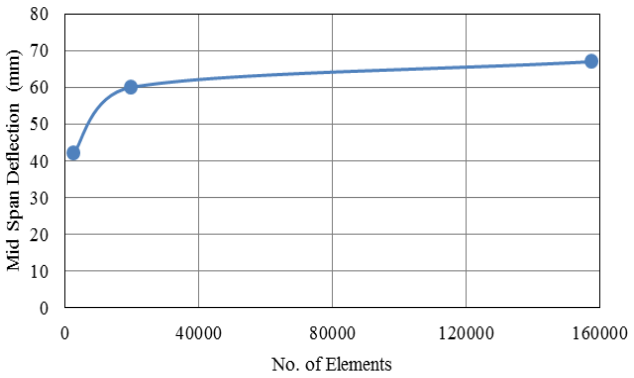

Fig. 6 Convergence of results study

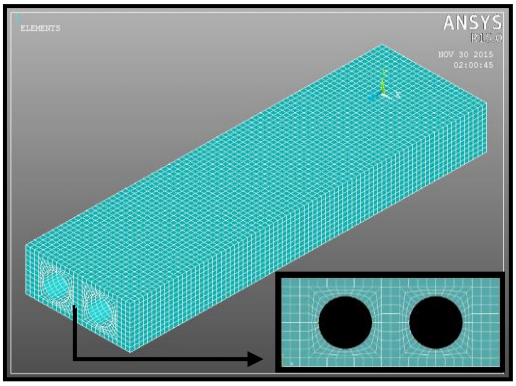

Fig. 7 Meshing of hollow-core slab (dia. 150 mm)

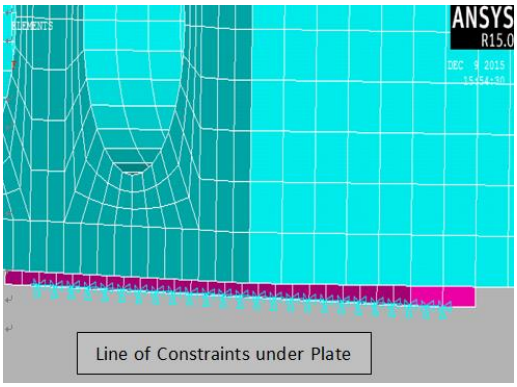

(a)

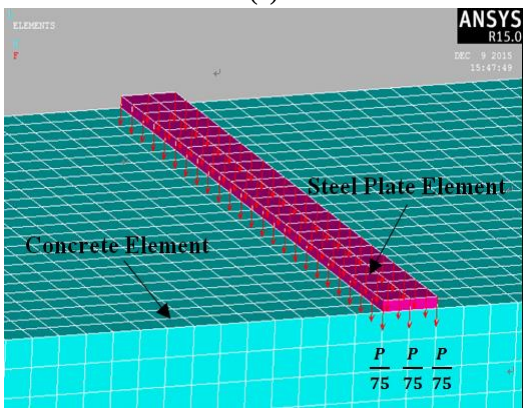

(b)

Fig. 8(a) Constraints of plate supports, (b) Distribution of applied load on nodes

(discrete model), so the two materials shared the same nodes.

• SOLID185 element was an eight node solid element having three degrees of freedom at each node translations in *x*, *y* and *z* directions. The element has capability of plastic deformation, hyperelasticity, stress stiffening, creep, large deflection, and large strain. In addition, the element has mixed nonlinear formulation that can be used for simulating deformations of nearly incompressible elastoplastic materials and fully incompressible hyperelastic materials. It was used for modeling steel supports. Steel plates were added at support and point of loading locations in the finite element models (as in the actual slabs) to provide a more even stress distribution over the support and point of loading areas. The steel plates were assumed to be linear elastic materials.

• PLANE182 element was used for 2-D modeling of solid structures. It was used for the area plane around the circular shape of slab cores only.

4.2 Modeling and meshing stages

The concrete model that represent the slabs with and without longitudinal hollow-cores are formulated using finite elements. The condition of symmetry is not used in the present study in order to compare the obtained results with the testing results of full experimental slab specimen. The formulation includes drawing areas at plan(*x*-*y*) in the first step and subtracts the cores areas and then extrudes them in (*z*-direction) to form the volume of the slabs. The net from longitudinal and transverse reinforcement bars which formed the reinforcement model was created through line element connected at the concrete element nodes to form perfect bond between steel bars and concrete elements.

As an initial and important step in the finite element modeling is the selection of the mesh density. A convergence of results is obtained when an adequate number of elements are used in a model. The slabs of same material properties, same loading and boundary conditions were modeled with an increasing number of elements for the concrete model. Three types of mesh of reinforced concrete slab (solid type) are used to find the best mesh size (2460, 19680 and 157440 elements) for element's size as (50, 25, 12.5 mm) respectively as shown in Fig. 5.

It can be concluded from Fig. 6 that the difference can be neglected when the number of elements increased from (19680) to (157440), therefore the (19680) model was adopted in the analysis of all slabs. After creating of volumes and selecting the size of mesh as (25 mm) for each concrete element, the model for all slabs are divided into (19680) elements by using (SOLID65) element type for concrete and after loading, stresses and strains are calculated at integration points of these small elements as shown in Fig. 6.

The meshing of concrete solid slab was done directly as cubic elements by (SOLID65) while the meshing of hollow-core slab with circular and square core shape need fine mesh for the area around the core opening in a way so that (SOLID65) element can be used for all slabs. The only way

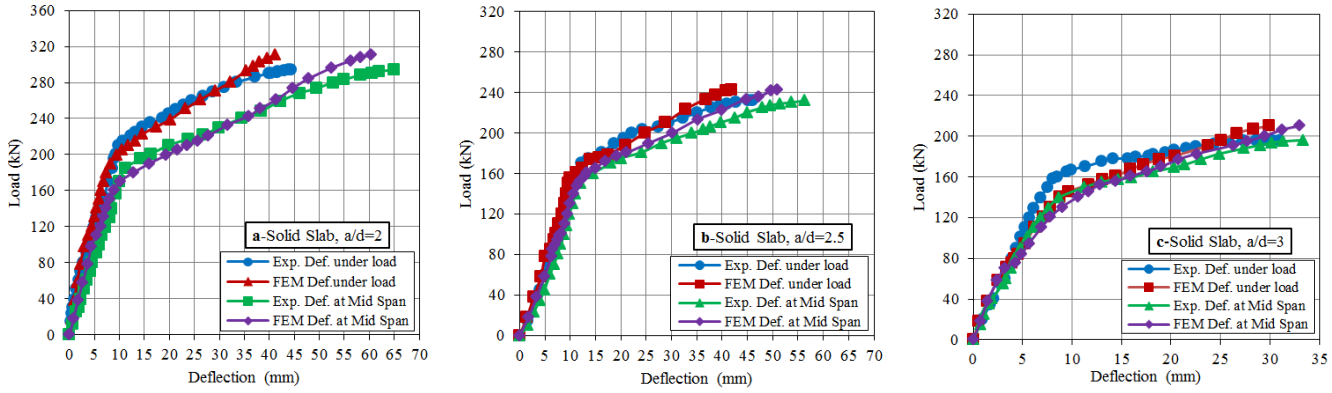

(a) (b) (c)

Fig. 8 Load deflection curves for solid slab (SS) with a/d (a)2, (b) 2.5, & (c) 3

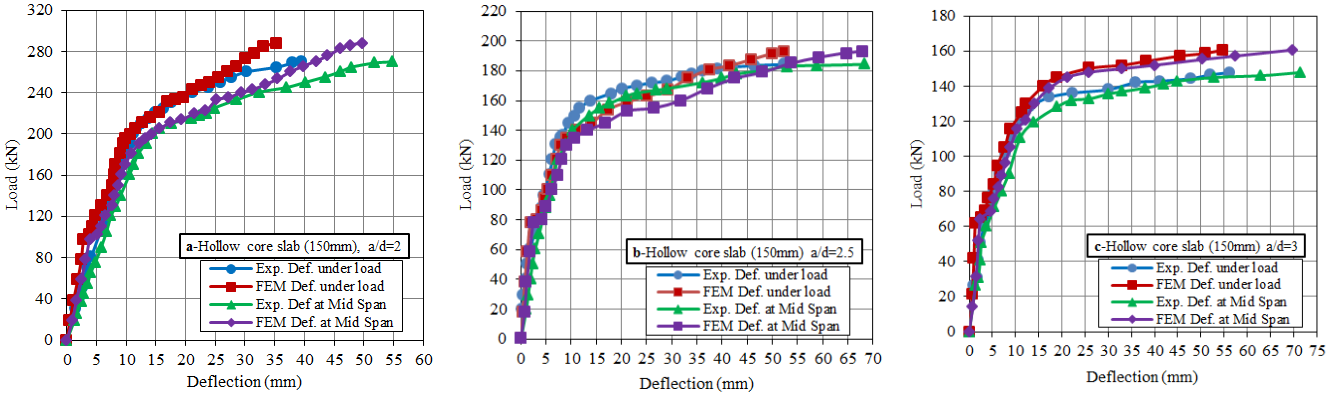

(a) (b) (c)

Fig. 9 Load deflection curves for hollow core slab (150 mm) (CCS) with a/d (a) 2, (b) 2.5 & (c) 3

Table 3 Materials properties of slab

Material model number	Element type	Materials properties	
1	SOLID65	Linear isotropic	
		Young's modulus	29385.5 MPa
		Poisson's ratio	0.2
		Multi-linear isotropic	
		Point No. Strain	Stress (MPa)
		Point 1 0.00039	11.43
		Point 2 0.001	25.6
		Point 3 0.0015	33.1
		Point 4 0.002	36.9
		Point 5 0.0026	38.1
		Concrete Properties	
		Open crack coefficient	0.8
		Closed crack coefficient	0.95
		Uniaxial cracking stress	3.40
		Uniaxial crushing stress	38.1
		Biaxial crushing stress	0
		Hydrostatic pressure	0
		Hydro biaxial crushing stress	0
		Hydro uniaxial crushing stress	0
		Tensile crack factor	0
2	LINK180 (Discrete)	Linear isotropic	
		Young's modulus	199100 MPa
		Poisson's ratio	0.3
		Bilinear isotropic	
		Yield stress	578 MPa
		Tang modulus	1991 MPa
3	SOLID185	Linear Isotropic	
		Young's modulus	2000000 MPa
		Poisson's ratio	0.3

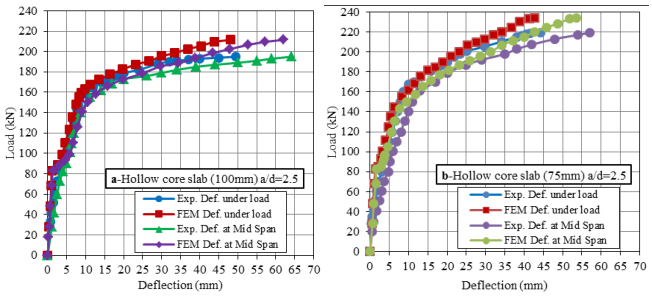

Fig. 10 Load deflection curves for hollow-core slab (CCS) with core diameter (a) 100 mm (b) 75 mm

to do that is by drawing symmetrizes four squares area to form a square area greater than the radius or the dimension of the core opening then drawing circle or square at the center of these square areas and subtract it to form the circular or square shape of core opening. The areas were limited between the out square area and voided circular or middle square shape will be meshed using concentrated meshes by (PLANE182) element then extrude it to be a volume and then meshing it with (SOLID65) element as shown in Fig. 7.

4.3 Loading and boundary condtions

The finite element models were loaded at the same locations of the tested slabs. In the experiment, the loading

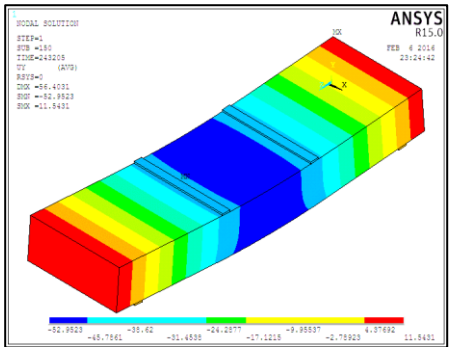

Fig. 11 Deflection contours (U_Y) of solid slab at ultimate load (a/d=2.5), (Slab-2)

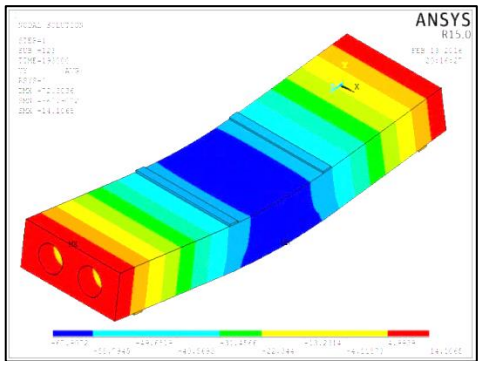

Fig. 12 Deflection contours (U_Y) of hollow core slab (150 mm), at ultimate load (a/d=2.5), (Slab-5)

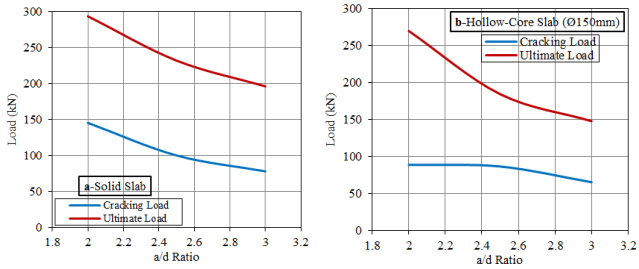

Fig. 13 Variation of (a/d) ratio with cracking and ultimate load for (a) Solid slab, (b) Hollow core slab (Ø 150 mm)

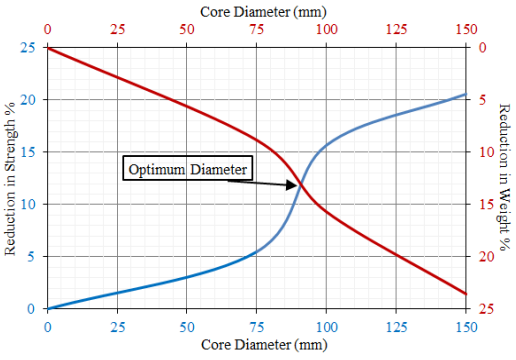

Fig. 14 Variation of core diameter with reduction of weight and strength

and support dimensions were approximately (50×600) mm. Two steel plates of (10 mm) thickness are modeled using (SOLID185) elements, were added at the support. The right steel plate was restrained in Z-direction (U_Z=0) and the left steel plate was restrained in X and Y direction (U_X=0, U_Y=0) with a single line of supports (see Fig. 8(a)).

Two steel plates at loading locations with the same size of concrete mesh in order to avoid stress concentration problems. This will provide a more even stress distribution over the support area. The external loads were applied on two steel plates over the surface of concrete slabs with the required locations. These loads were applied in the form of concentrated loads on all top nodes of plates (75 node per plate) as a ($\frac{P}{75}$) for each node as shown in Fig. 8(b) to simulate the real loads which adopted in the experimental work. The application of the loads up to failure was done incrementally as required by the Modified Newton-Raphson method. Therefore, the total applied load is divided into a series of load increments (load step). Within each load step, maximum of (200) iterations were permitted.

Table 4 Test results of slabs

Slab type	Slab no.	$\frac{a}{d}$	Load (kN)		$\frac{P_{cr}}{P_u}$ × 100 %	Deflection (mm)		Mode of failure
			Cracking load (P_{cr})	Ultimate load (P_u)		Deflection at cracking load (Δ_{cr})	Deflection at ultimate load (Δ_u)	
Solid	Slab-1	2	145.50	293.76	49.5	8.560	64.87	Flexural-shear
	Slab-2	2.5	100.23	232.05	43.1	8.822	56.28	Flexural
	Slab-3	3	78.10	196.34	39.8	4.143	33.38	Flexural
Hollow core 150 mm	Slab-4	2	88.76	269.89	32.9	5.610	54.79	Flexural-shear
	Slab-5	2.5	86.47	184.31	46.9	4.811	68.38	Flexural-shear
	Slab-6	3	65.23	147.85	44.1	4.647	71.52	Flexural-shear
Hollow core 100 mm	Slab-7	2.5	90.21	195.65	46.1	5.03	64.25	Flexural-shear
Hollow core 75 mm	Slab-8	2.5	100.02	219.31	45.6	5.84	56.98	Flexural

Table 5 Comparison the of experimental and finite element results

Slab type	Slab no.	Ultimate load (kN)				Ultimate deflection (mm)		
		Exp. (P_u)	FEM (P_u)	Diff. %	$(P_u)_{Exp.}$ / $(P_u)_{FEM}$	Exp. (Δ_u)	FEM (Δ_u)	Diff. %
Solid	Slab-1	293.76	310.60	5.73	0.946	64.87	60.43	6.84
	Slab-2	232.05	243.21	4.81	0.954	56.28	52.95	5.92
	Slab-3	196.34	210.19	7.05	0.934	33.38	33.02	1.08
Hollow core 150 mm	Slab-4	269.89	288.28	6.81	0.936	54.79	49.69	9.31
	Slab-5	184.31	193.00	4.71	0.955	68.38	67.91	0.69
	Slab-6	147.85	160.690	8.68	0.871	71.52	69.87	2.31
Hollow core 100 mm	Slab-7	195.65	211.50	7.49	0.925	64.25	62.92	2.08
Hollow core 75 mm	Slab-8	219.31	234.00	6.69	0.937	56.98	53.50	6.10

4.4 Model parameters

The finite element models adopted in this study have a number of parameters which can be classified into three categories as shown in Table 3.

1. Concrete property parameters
2. Steel Reinforcement property parameters
3. Steel Plate property parameters

5. Experimental and numerical results

Experimental

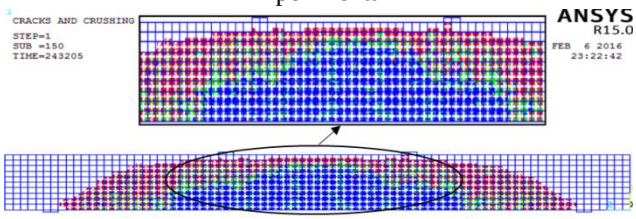

Finite element analysis

Fig. 15 Crack pattern at ultimate load for (Slab-2)

Experimental

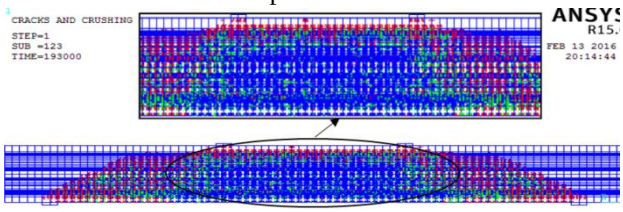

Finite element analysis

Fig. 16 Crack pattern at ultimate load for (Slab-5)

Experimental

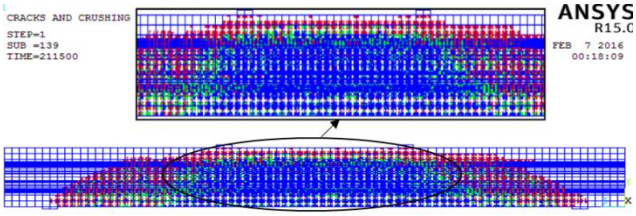

Finite element analysis

Fig. 17 Crack pattern at ultimate load for (Slab-7)

Experimental work and numerical solution (i.e., finite element method) results which are obtained are presented and then discussed. Experimental measurements which are carried out by testing eight slabs including the ultimate loads, load-deflection curves are given. Comparisons between the experimental and the numerical results are made to verify the application of the suggested numerical idealization on the tested slabs. ANSYS program was used to analyze the same slabs and study the effect of some additional parameters on the behavior of these slabs.

Experimental

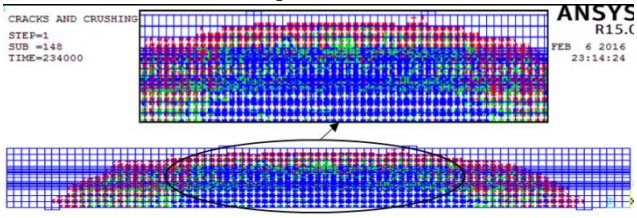

Finite element analysis

Fig. 18 Crack pattern at ultimate load for (Slab-8)

5.1 Load-deflection curves

The deflection (vertical displacement) in *Y*-direction (UY) are obtained at the center of mid span and under the load of the bottom face of the slab. The load versus deflection plots obtained from the numerical and the experimental study are presented for comparison in Fig. 8 to Fig. 10. Deflection contour of finite element analyzed slabs due to the applied loading is shown in Fig. 11 and Fig. 12.

In Fig. 13, the comparison presents between solid and hollow-core slab with core diameter (150 mm) by variation (a/d) ratio with cracking and ultimate load. It was concluded that increasing (a/d) ratio the cracking load and ultimate load will be decrease identity for solid slab but the cracking load in hollow core slab decreases with low rate up to (a/d) ratio 2.5.

The selection of optimum core diameter presents in Fig. 14 by comparison the core diameter with reduction of weight and reduction of strength. The curves are intersecting in optimum core diameter (91 mm) in which the reduction in weight equals the reduction in strength. The obtained optimum core diameter can be used for the slab scale 1:2 only and it will be change if the scale changed to 1:1 but the ratio of cores area to total section area remains the same.

5.2 Loads at failure

The test results are presented in Table 4. In this Table, the mode of failure for each slab depends on monitoring the cracking paths during applying the loads until failure stage and based on which crack is the dominant. A comparison between the ultimate loads of the experimentally tested slabs $(P_u)_{Exp}$ at failure stage and the final loads obtained from finite element models $(P_u)_{FEM}$ is shown in Table 5. The final loads for the finite element models are the last applied loads before the solution starts to diverge due to numerous cracks and large deflection in *Y*-direction (UY). The ultimate loads obtained from numerical models are in excellent agreement with the corresponding values from the experimentally tested slabs. The numerical results show that greater ultimate load with smaller deflection at the ultimate load stage as compared to experimentally results.

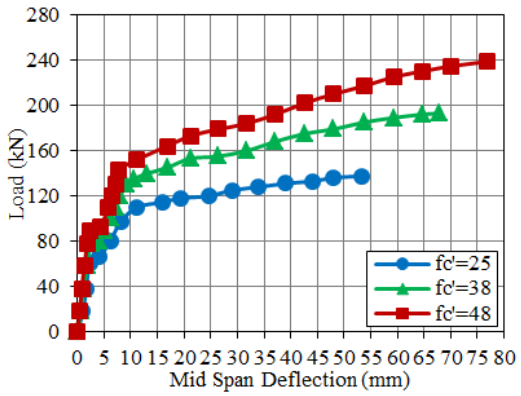

Fig. 19 Effect of concrete compressive strength on the behavior of hollow core slab with 150 mm core size

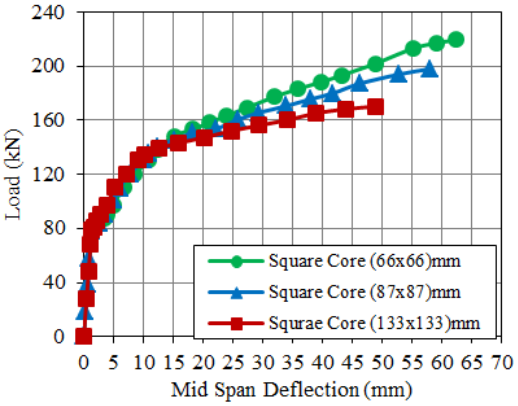

Fig. 20 Effect of core size on the behavior of hollow core slab with square core shape

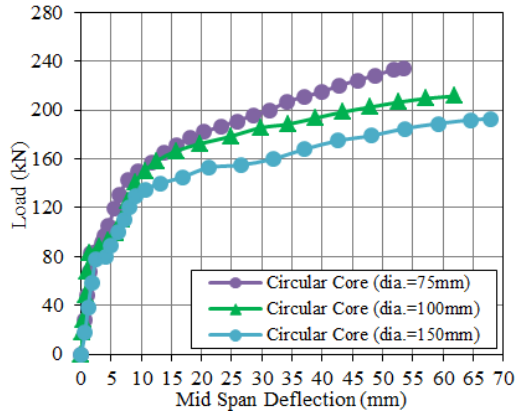

Fig. 21 Effect of core size on the behavior of hollow core slab with circular core shape

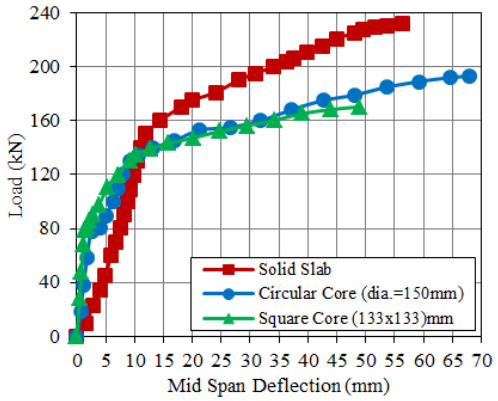

Fig. 22 Effect of core shape on the behavior of hollow core slab

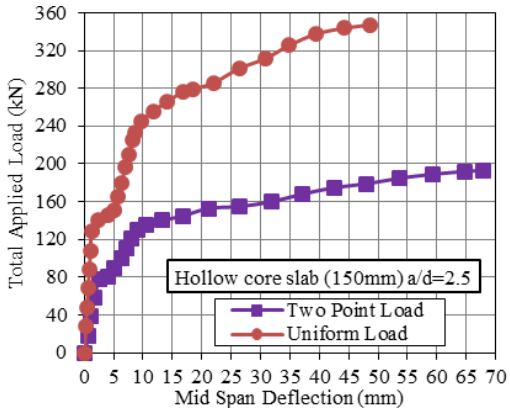

Fig. 23 Effect of loading type on the behavior of hollow core slab

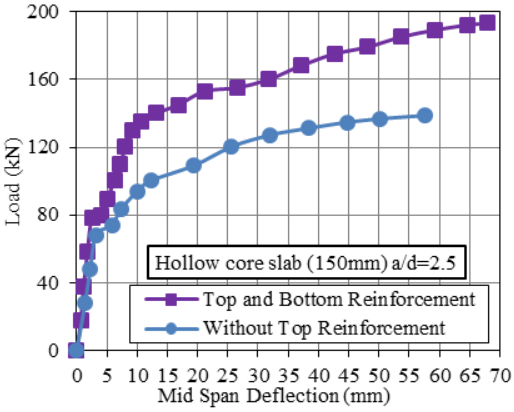

Fig. 24 Effect of removing top steel reinforcement on the behavior of hollow core slab

5.3 Crack pattern

As expected, the main cracks for all tested slabs commenced at middle third (flexural cracks) from the bottom face as a line with the width of the slab and all slabs exhibited ductile flexural failure. It was noted that some of shear cracks appeared in slabs which tested with (a/d) ratios (2 and 2.5) especially in hollow-core slab due to position of applied loads and presence the holes of hollow-core slab but the failure of these slabs are flexural failure. ANSYS computer program displays circles at locations of cracking or crushing in concrete elements. Fig. 15 to Fig. 18 show the location of cracks from experimental test and finite element analysis along the solid and hollow-core slabs with core diameter (150, 100 and 75) respectively.

6. Parametric study

The parameters that may affect the behavior of the hollow-core reinforced concrete slabs under the same conditions and not tested are studied here in:

6.1 Effect of compressive strength of concrete

The reinforced concrete hollow-core slab having core diameter (150 mm) under (a/d) equal 2.5 was selected to study the influence of the grade of concrete on the behavior of load-deflection curve. It has been reanalyzed using different values of concrete compressive strength as (25, 38, and 45) MPa respectively (This means increasing the stiffness of concrete). The Fig. 19 shows the response of the considered R.C hollow-core slab for different concrete compressive strength.

6.2 Effect of shape and size of hollow cores

The hollow core slabs having circular core shapes and square core shapes were analyzed with equivalent areas of three sizes for each core shape under same loading and support conditions. The circular shape types were presented and analyzed previously while the equivalent square core shapes having dimensions (133×133 mm, 89×89 mm and 66×66 mm). The analysis results (load-deflection) curves and comparison with sizes and shapes of hollow cores were presented at Figs. 20, 21 and 22.

6.3 Effect of loading type

The reinforced concrete hollow-core slab with circular core (diameter 150 mm) was analyzed under uniform load on all surface nodes of the concrete elements by ANSYS program. The analysis results compared with the results of the same slab under two point loads with the ratio (a/d=2.5). The results indicate that the ultimate total load of this slab was increased from (193 kN) for two point loads to (347 kN) under uniform load type with decreasing in deflection by about (28.5%) as shown in Fig. 23. It can be seen from this figure that the polyline appeared clearly in load-deflection curve for load values between 120 kN and 160 kN which refers to the transformation stage of numerical solution from linear to non-linear behavior (cracking occur).

6.4 Effect of top layer of reinforcement

Fig. 24 shows the effect of using top steel reinforcement with bottom one. The hollow-core slab with core diameter (150 mm) under two-point loading with (a/d) equal 2.5 was analyzed first with top and bottom reinforcement as presented before then analyzing the same slab with removing the top reinforcement. It was noted that the ultimate load capacity of the slab will decreased by about 28% with removing the top reinforcement. This is may be due to the existence of top reinforcement will distribute the stresses around the core and prevent crushing.

7. Conclusions

Based on the analysis results of the experimental and numerical investigations of the solid and hollow-core slabs, the following conclusions can be drawn:

• The cracking and ultimate strength of the moderately thick solid and hollow-core slab lead to be decreased with increasing the diameter of the cores and also with increasing the ratio of shear span to effective depth (a/d).

• Reducing the own weight of the moderate thick reinforced concrete slabs by about 23.6% with longitudinal hollow cores (dia.=150 mm) lead to reduce the ultimate strength by about 20.6% while reducing the weight by about 15.71% with hollow cores (dia.=100 mm) lead to reduce the ultimate strength by about 15.68% and reducing the weight by about 8.84% with hollow cores (dia.=75 mm) lead to reduce the ultimate strength by about 5.49%.

• Increasing the ratio (a/d) from 2 to 3 lead to reduce the ultimate strength by about 33% in solid slab with decreasing the deflection. While 45% reduction in ultimate load fore hollow-core slab with increasing the deflection due to reducing the stiffness of slab with removing the concrete volume of hollow cores.

• In hollow-core reinforced concrete slab, the circular core shapes have cracking and ultimate strength greater than the square shape by about 13.4% and increasing in deflection by about 39.5%. The increase in core size for circular core shape caused a reduction in ultimate strength with increasing the deflections while increasing the core size in square core shape cause a reduction in ultimate strength with reducing deflections.

• When the compressive strength of the concrete increases from (38 MPa) to (48 MPa), the ultimate strength increase by 23.6% and when the compressive strength decrease from (38 MPa) to (25 MPa), the ultimate strength reduces to about 28.7%.

• It was found that the ultimate strength of the hollow-core slab increases by about 80% for the case of uniform load and a reduction in deflection by (28.5%) compared to two point loads with (a/d) equal 2.5.

• It was concluded that removing the top steel reinforcement in hollow-core slab reduces the ultimate strength by about 28% due to crushing failure of top flange of concrete so that it is recommended to use this layer prevent this failure.

• Results of comparison between experimental and finite element results show that the difference range was (4.71-8.68)% in ultimate load and (0.69-9.31)% in deflection.

• It is recommended that the optimum core diameter in hollow-core slab for scale 1:2 is (91 mm) because of that the reduction in weight and strength are equal. In addition, reducing the core diameter will increase the ribs and that cause increasing in strength of the slab.

References

ACI318-14 (2014), *Building Code Requirements for Structural Concrete (ACI 318-14) and Commentary*, Detroit, U.S.A.

ANSYS 15.0 Inc (2013), *ANSYS User's Manual*, SAS IP, Inc., Version 15.0, U.S.A.

Brunesi, E., Bolognini, D. and Nascimbene, R. (2014), "Evaluation of the shear of precast-prestressed hollow core slab: Numerical and experimental comparison", *Mater. Struct.*, **48**(5), 1503-1521.

Chang, J., Buchanan, A.H., Dhakal, R.P. and Moss, P.J. (2008), "Simple method for modeling hollow core concrete slabs under fire", University of Canterbury, New Zealand.

Hai-tao, L., Deeks, A., Liu, L., Huang, D. and Su, X. (2011),

"Moment transfer factors for column-supported cast-in-situ hollow core slabs", *J. Zhejiang Univ*., **13**(3), 165-173.
Haruna, S.I. (2014), "Flexural behavior of precast pre-stressed concrete hollow core slabs with cast-in-place concrete topping", M.S. Dissertation, Atılım University, Turkey.
Lee, D.H., Park, M., Oh, J., Kim, K.S., Im, J. and Seo, S. (2014), "Web-shear capacity of prestressed hollow core slab unit with consideration on the minimum shear reinforcement requirement", *Comput. Concrete*, **14**(3), 211-231.
Pajari, M. (2004), *Pure Torsion Tests on Single Hollow Core Slabs*, Espoo VTT Tiedotteita, Research Notes 2273, 29-28.
Rahman, M.K., Baluch, M.H., Said, M.K. and Shazali, M.A. (2012), "Flexural and shear strength of pre-stressed precast hollow-core slabs", *Arab. J. Sci. Eng*., **37**(2), 443-455.

CC